Adsorption of imidazole on Au(111) surface: Dispersion corrected density functional study

Safia Izzaouihda[1], Khaled Mahjoubi[2], Hassna Abou El Makarim[1], Najia Komiha[1], David M. Benoit[3]

[1]LS3ME-Faculté des Sciences, Université Mohammed V Rabat Morocco
[2]LSAMA- Faculté des Sciences, Tunis Al Manar, Tunisia
[3]Department of Chemistry, University of Hull, UK

Abstract

We use density functional theory in the generalized gradient approximation to study the adsorption of imidazole on the Au(111) surface and account for dispersion effect using Grimme's empirical dispersion correction technique. Our results show that the adsorption energy of imidazole depends on the slab size and on the adsorption site. In agreement with other studies, we find the largest adsorption energy for imidazole on a top site of Au(111). However, we also note that the adsorption energy at other sites is substantial.

Keywords: imidazole, interaction, Au(111) surface, adsorbed sites, DFT, DFT-D3, zeolitic imidazole framework (ZIF).

1. Introduction

In the present study, we investigate the interaction between imidazole and the Au(111) surface. This surface is often used in experimental investigations as it is easy to prepare and clean using standard annealing methods and sputtering techniques (see ref.[1] for example), making it an ideal prototype metal substrate. The interaction of imidazole building blocks with metal surfaces is also of particular interest to the zeolite community as there has been a growing trend in coupling porous materials, such as zeolitic imidazolate frameworks (ZIFs), with metallic supports to create a new type of functional materials.[2,3] These meta-materials are developed to improve on the current properties of ZIFs for gas separation,[4,5] gas storage[6] and catalysis.[7]

In this paper, we explore the applicability of two slab models for the Au(111) surface and investigate the adsorption of an imidazole molecule using periodic density functional theory (DFT) in the Gaussian plane wave pseudo potential formalism. More specifically, we assess the impact of large unit cells to evaluate the effectiveness of Γ-point only calculations for metal surfaces, as those

are often seen in the literature for a number of periodic DFT programs. Increasing the unit cell is a computationally more expensive alternative to the use of k-points but offers a simple conceptual approach that can be applied to any periodic code. We also investigate the adsorbate image interaction effect that is often pervasive in all periodic DFT adsorption calculations but that is traditionally neglected in most studies.

Finally, even though pure DFT calculations have greatly contributed to understanding interaction between adsorbate molecule and surfaces, it is vital to include dispersion effects in order to take into account the weak forces at play that can prove to be significant. In this study we choose to use Grimme's latest empirical dispersion correction scheme (DFT-D3),[8] as implemented in the CP2K/Quickstep module.[9]

This paper is organised as follows: we describe the details of our computational approach in section 2 and present our results in section 3. This section is divided in three parts: section 3.1 discusses our two models for the Au(111) surface, section 3.2 reports our DFT and DFT-D3 calculations for adsorbed imidazole on Au(111) and section 3.3 shows an analysis of the charge density difference between imidazole and the surface. We present our conclusions in section 4.

2. Computational methods

Calculations are performed using the QUICKSTEP module[9] tightly integrated in the CP2K program package.[10] The QUICKSTEP module is a very efficient implementation of density functional theory (DFT)[11,12] using a hybrid Gaussian and plane wave method (GPW).[13] This implementation allows an efficient treatment of electrostatic interaction and leads to a linear scaling of the computational time for the total energy with respect to system size. QUICKSTEP uses Geodecker–Teter–Hutter (GTH)[14] relativitic pseudo potentials, which provide a compact and efficient description of the core electrons. The GTH pseudo potentials are generated using fully relativistic all-electron calculations for each atom.

Otherwise, we use the generalized gradient approximation (GGA) to treat exchange-correlation effects in the form of the Perdew–Burke–Ernzerhof (PBE) functional.[15] For each atom, we use the TZV2P-MOLOPT-GTH[16] basis set, except for Au where we use the DZVP-MOLOPT-GTH[16] basis set. We use the orbital transformation method (OT)[17] to minimise the total ground state energy. All calculations were performed at the Γ-point of the Brillouin zone. The two-dimensional periodic boundary conditions are applied in two directions x and y (i.e., no periodicity along z direction). The BFGS optimisation method has been used for all the calculations with an energy convergence

criterion of 10^{-7} Hartree and a largest force allowed upon geometrical relaxation of 4.5 10^{-6} Bohr/Hartree.

Furthermore, to improve the description of long-range dispersion interactions, we use an empirical vdW correction of the DFT energy as suggested by Grimme[8] in his revised DFT-D3 approach. Using this dispersion correction, the total energy is obtained as a sum of the self-consistent Kohn-Sham total energy, E_{KS-DFT}, and the dispersion correction expressed as a sum of two- and three-body energies, $E_{dis} = E^{(2\,body)} + E^{(3\,body)}$, therefore:

$$E_{DFT-Da} = E_{KS-DFT} + E_{dis}$$

Note that the correction depends primarily on the inter-nuclear distance between all atom pairs in the system.

3. Results and discussion

3.1. Au(111) surface models

Our two model surfaces are based on a unit cell of three (111) layers (12 Au atoms per layer) with a vacuum of five layers along the *z*-axis; the uppermost layer is allowed to relax in the calculation, but the lower two layers are kept fixed. M. Mavrikakis *et a.l*[18] have investigated particle-size-dependent gold reactivity and found that the adsorption energy of small molecules (O and CO) does not depend on the number of Au layers if there are more than two layers present in the simulation.

The lattice constant used to generate our model is that calculated at the PBE/PAW Level of theory by Dal Corso,[19] $a_0 = 4.1628$ Å.

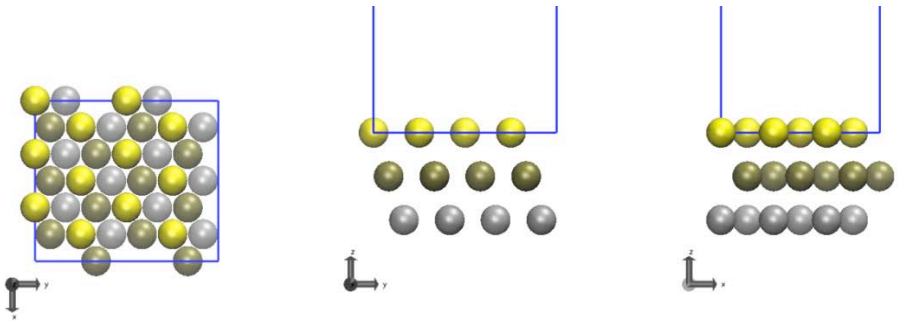

Fig. 1 Top and side view of our Au(111) surface model. Yellow, tan and silver colour represent the top, second and third Au(111) layer, respectively.

Fig.1, show the initial geometry that has been chosen for the smaller Au(111) surface model: A slab of three layers with 12 Au atoms per layer. Careful testing of the effect of the density cut off energy on the total energy is shown in Fig.2. We find that 500 Ry is suitably close to convergence

for our calculation of the Au(111) surface while keeping the computational cost manageable. Note that this is also valid for our larger 30 atoms/layer model.

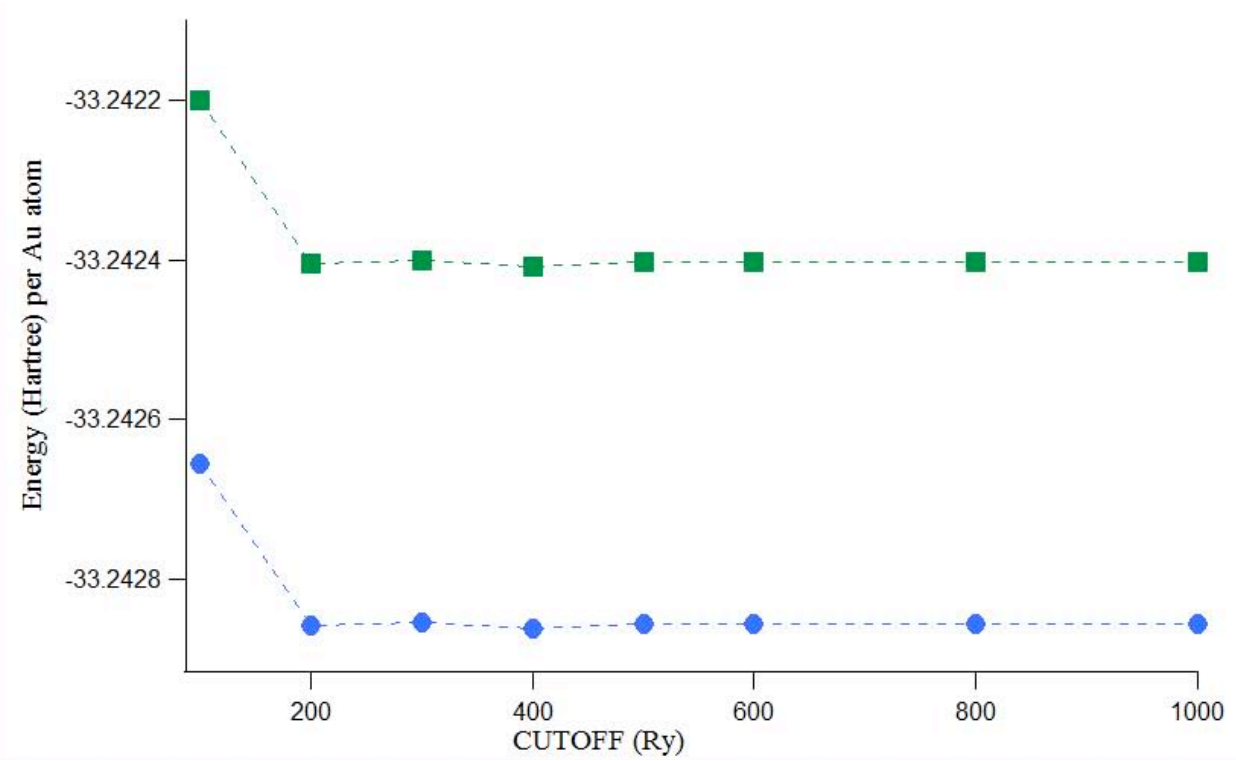

Fig. 2 Energy per atom of our Au(111) surface models as a function of the density cut off energy. Blue and green colour represent the Au(111) small surface of model 12 atoms/ layer and the Au(111) larger surface model of 30 atoms/layer respectively.

Using Dal Corso's lattice constant, we compute an ideal bulk inter-atomic distance ($d_{\text{Au-Au}}$) of 2.95 Å since for a cubic closed packed lattice we have: $d_{\text{Au-Au}} = \frac{1}{\sqrt{2}} a_0$

The geometry optimisation of the initial geometry of the Au(111) model surface results in a planar zigzag arrangement of gold atoms in the relaxed layer, as can be seen from Fig.3. This bond alternation effect is likely caused by symmetry breaking[20] and lack of k-point sampling.

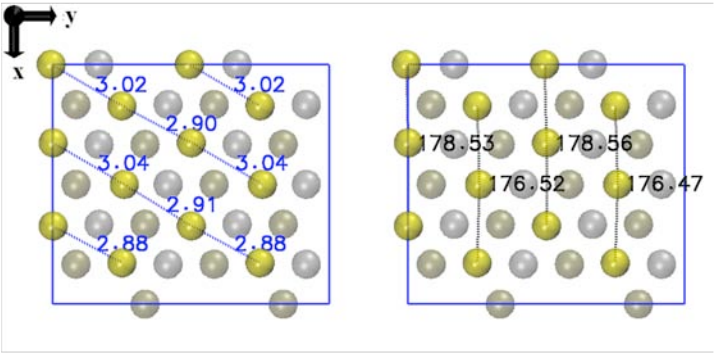

Fig. 3 *Au–Au bond length and Au–Au–Au angles for the relaxed top layer of our Au(111) surface model. Yellow, tan and silver colour represent the top, second and third layer, respectively.*

In order to reduce any intrinsic surface stress observed in the relaxed layer of our initial Au(111) surface model, we create a $2 \times 2 \times 1$ supercell (increasing *xy* directions only) which generates a slab model with 30 atoms per layer. This second surface model is shown in Fig.4.

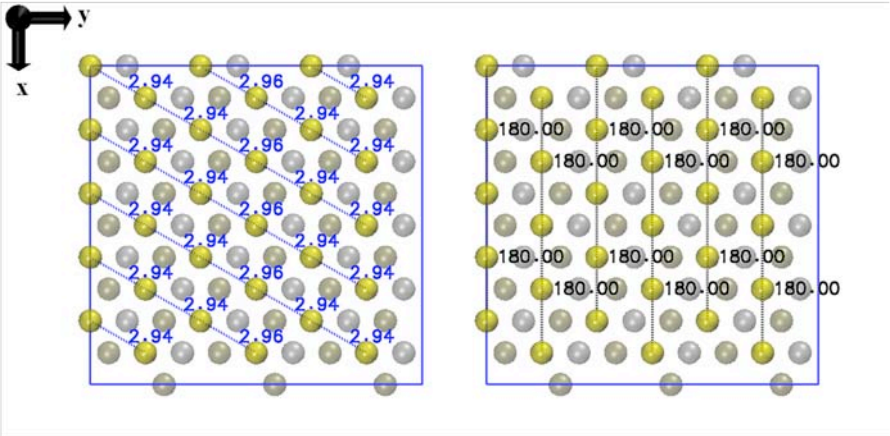

Fig.4 Optimised geometry of the second Au(111) surface model with 30 atoms per layer. Note that only the top layer is relaxed while the other two layers are kept fixed.

The extended $2 \times 2 \times 1$ surface model is more regular and does not present any significant bond length alternation, unlike the smaller surface model (see Fig. 3 and Fig. 4). We observe that moving from a 12 atoms/layer model to a 30 atoms/layer model enables the top layer to relax to a regular array of Au atoms with consistent inter-atomic distances that are in good agreement with what would be expected from the computed bulk lattice constant. Thus increasing the number of atoms leads to a much more suitable Au surface model, despite performing Γ-point only calculations.

3.2. Adsorbed imidazole molecule on the Au(111) surface

We investigate the suitability of each Au(111) surface model for describing interactions with adsorbents by considering the adsorption energy of the imidazole molecule. This is also of importance for catalysis, as for surface reactions there is usually a close correlation between binding energies and activation energies.[21,22] For the imidazole molecule, the lone pair of the deprotonated nitrogen atom that is not involved in the aromatic system is the most reactive site[23,24] and thus the most likely site to bind to Au.

After optimising the imidazole/Au(111) interface (both adsorbate and first Au layer), we obtain an N–Au distance of 2.30 Å for the smaller Au(111) surface model (12 atoms/layer) shown in Fig.5.

This distance is in agreement with the results obtained by Iori *et al.*[25] ($d_{N–Au}$ = 2.30 Å) who used a similar 12 atoms/layer model along with the PBE exchange–correlation functional, ultra-soft pseudo potentials and 4x4x1 k-point sampling. We note that, in our model, the Au atom interacting with imidazole moves out of plane from its initial position by 0.05 Å.

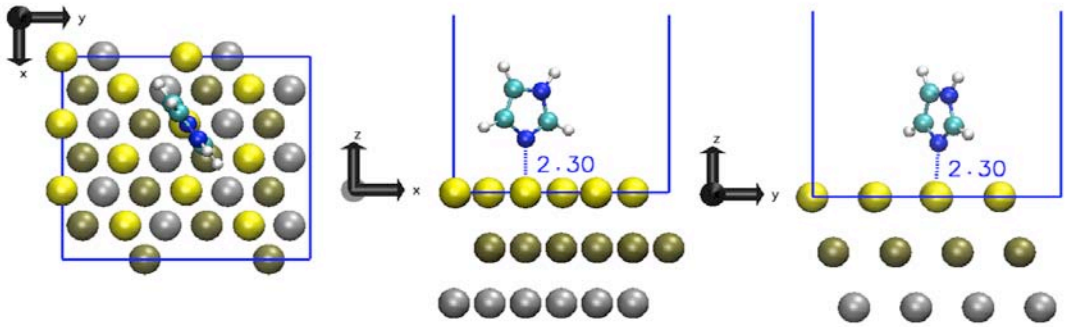

Fig.5 Top and sides views of the optimised geometry of imidazole/Au(111) for the smaller 12 atoms/layer model: the N atom is above a top site of the 111 surface and is one-fold coordinated.

We then perform a similar optimisation for imidazole adsorbed on the larger Au(111) surface model (30 Au atoms/layer) and obtain again an N–Au distance of 2.30 Å, in perfect agreement with the smaller surface model and Iori *et al.*.[25] However, this time the Au atom interacting directly with imidazole only slightly displaced out of plane (0.02 Å) for the larger surface model. The resulting adsorption geometry is shown in Fig.6.

For both surface models, the N–Au distance is slightly longer than the sum of the corresponding covalent radii, $r_{cov}^{N} + r_{cov}^{Au} = 0.71 + 1.36 = 2.06$ Å ,[26] and considerably shorter than the sum of the van der Waals radii, $r_{vdw}^{N} + r_{vdw}^{Au} = 1.55 + 1.66 = 3.12$ Å .[27]

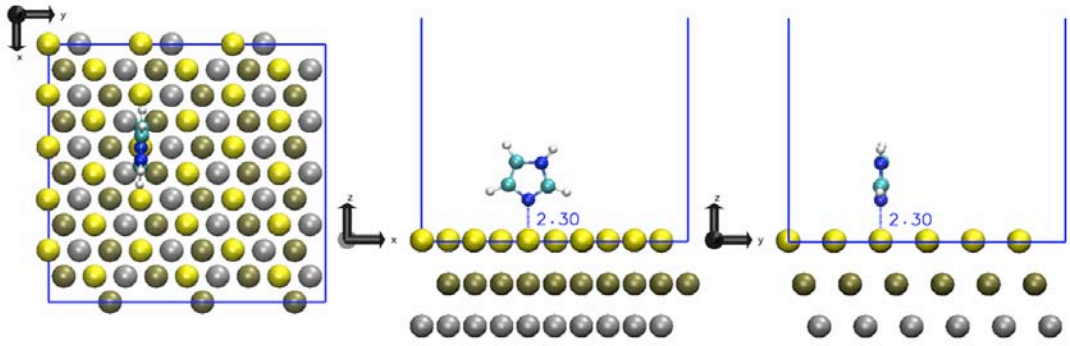

Fig.6 Top and side views of the optimised geometry of imidazole/Au(111) for the larger 30 atoms/layer surface model: the N atom is above a top site of the 111 surface and is one-fold coordinated.

We compute the adsorption energy, E_{ads}, for the imidazole molecule (Im) on the Au(111) surface as follows:

$$E_{ads} = E_{\mathrm{Im@Au(111)}} - E_{\mathrm{Im}} - E_{\mathrm{Au(111)}}$$

where $E_{\mathrm{Im@Au(111)}}$ is the total energy for the optimised adsorbed imidazole molecule on the relaxed Au(111) surface model, E_{Im} is the total energy of the optimised isolated imidazole and $E_{\mathrm{Au(111)}}$ is the total energy of the optimised clean Au(111) surface. We obtain an adsorption energy of –71.59 kJ mol^{-1} and –73.98 kJ mol^{-1} for the small and large slab model, respectively. Our adsorption energies are about twice as large as the value computed by Iori *et al.*[25] (–45.6 kJ mol^{-1}) but the latter was computed without accounting for relaxation of the isolated systems. Another difference is that Iori *et al.* did not impose any constraints on the position of the Au atoms in the layers during optimisation, however is usually recommended that at least one layer is kept frozen to maintain bulk structure (see for example the method outlined in ref.[28]). Finally, it is also worth noting that our calculations use an atom-centerer basis set which could also lead to basis set superposition error (BSSE) in the calculation of adsorption energy. However, the basis set we used (MOLOPT-GTH[16]) is designed to limit the extent of BSSE but yet does not completely remove BSSE contributions in the computed adsorption energy. This could also explain our larger adsorption values compared to those determined using a plane-wave technique, for example.

As an alternative point of comparison, Kovacevic and Kokalj[28] computed an adsorption energy of similar magnitude (–66.57 kJ mol^{-1}) for imidazole adsorbed on Cu(111) using the PBE exchange–correlation functional, ultra-soft pseudo potentials and a plane waves basis set with 30 Ry cut off energy. While adsorption on a Cu(111) surface does not behave identically to an Au(111) surface, it has been shown that adsorption energy on both surfaces is similar for benzene at the dispersion corrected DFT level of theory.[29]

We also observe that the adsorption energy determined using the 30 atoms/layer slab model is slightly larger than that determined using the 12 atoms/layer model. One interesting point is that the orientation of the adsorbed imidazole molecule changes with the size of the slab model. This is apparent if we compare Fig. 5 to Fig. 6, as the imidazole molecule is at a –45˚ tilt with respect to the a cell vector for the 12 atoms/layer slab model but is parallel with the a cell vector for the larger 30 atoms/layer model. This change of orientation is likely due to lateral dipole-dipole interactions caused by the large dipole moment of the imidazole molecule. This type of interactions is very effective at long-range and can influence nearest neighbours over several Angstroms.[28] To illustrate the close proximity of imidazole images in connection with this point, we show in Fig.7 the electron density of the system using two different isosurface values. We see that for an isovalue of 0.025 e Å^{-3} both slab models exhibit a similar density distribution around the imidazole molecule apart from

the –45° tilt mentioned earlier for the small slab model. When we decrease the value of the isosurface to 10^{-5} *e* Å^{-3}, we notice that the electron density of the imidazole molecule adsorbed on the small slab model is perturbed/influenced by the presence of its image in the neighbouring cells. This is evidenced by the "open" isosurface (see Fig. 7 bottom left) that indicate that there is a small degree of sharing of the adsorbed imidazole molecule with its own image in the next cell. This is not the case for the large model (see Fig. 7 bottom right) where the density isosurface of adsorbed imidazole molecule completely covers the molecule, thus indicating that there is less image-induced perturbations in this system. This observation correlates with our earlier remark regarding the long-range dipole interactions that could influence adsorbate orientation for small slab models.

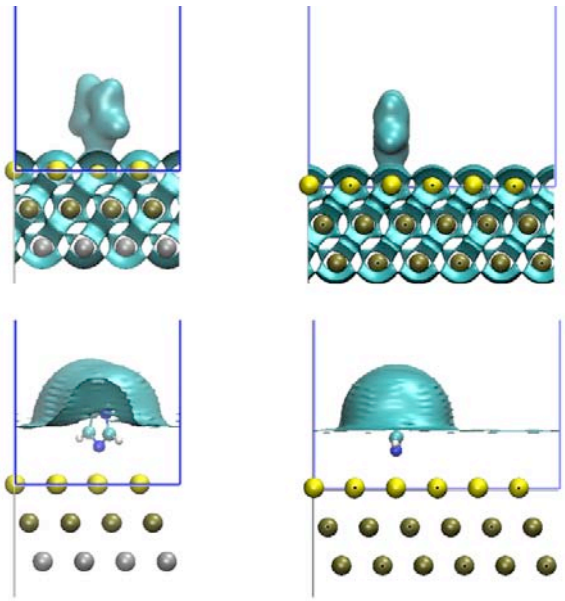

Fig.7 Electronic density of imidazole molecule on top-site of both Au(111) slab models. Smaller slab model (12 atoms/layer) on the left and larger slab model (30 atoms/layer) on the right. The upper panel shows the density for an isovalue of 0.025 e Å^{-3} and the lower panel an isovalue of 10^{-5} e Å^{-3}

In order to assess the site preference of imidazole on Au(111) and the influence of the size of the slab model on energetic ordering, we optimise the structure of imidazole/Au(111) with starting geometries at various the possible adsorption sites on the Au(111) surface, namely: top, bridge, FCC and HCP sites (se also Fig.8).

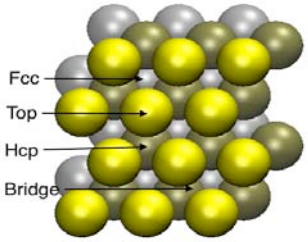

Fig.8 Top view of four low energy adsorption sites of the Au(111) surface.

To aid the convergence of the geometry optimisation, the deprotonated nitrogen atom of the imidazole molecule is only allowed to move perpendicularly to the Au(111) surface (*z* direction only) while its *x* and *y* positions are fixed to be above top, bridge, FCC and HCP sites in turn. Our adsorption energies for both slab models are shown in the first two lines of Table 1.

		Adsorption energy [kJ mol^{-1}]			
Method	**Surface Model**	**Top**	**Bridge**	**FCC**	**HCP**
PBE	12 Au/layer	–71.60	–42.64	–35.45	–37.04
	30 Au/layer	–73.97	–43.42	–36.79	–37.73
PBE-D3	12 Au/layer	–112.42	–85.84	–74.35	–76.75
	30 Au/layer	–117.04	–84.92	–74.16	–76.94

Table 1 Adsorption energy of imidazole at top, bridge, FCC, and HCP sites on the Au(111) surface. The calculations use a small (12 atoms/layer) and a large (30 atoms/layers) surface model along with the PBE exchange–correlation functional without or with dispersion corrections (PBE-D3).

We see that, for the pure PBE functional, the top site has the largest adsorption energy (–73.97 kJ mol $^{-1}$) and the larger surface model is slightly more binding than the small surface model. This trend is maintained for the other adsorption sites despite their binding energies being about half that of the top site. The energetic ordering of the adsorption sites is top > bridge > HCP > FCC for both small and large models. The slight increase of adsorption energy with the number of Au atoms in each layer is in agreement with the results found by Kovacevic and Kokalj,[28] who studied the influence of dipole-dipole interaction of several azoles on Cu(111) and Al(111) surfaces. Indeed, they report that the adsorption energy of imidazole is a function of the nearest neighbour distance and that their computed adsorption energy becomes more negative as this distance increases.

As mentioned earlier, long-range interactions play an important role in the adsorption energetics of the imidazole molecule on the Au(111) surface and thus an appropriate treatment of van der Waals forces is necessary for a correct description of adsorption. The DFT-D3 dispersion correction method[8] is currently one of the most popular techniques to account for weak interactions in molecular systems due to its negligible computational cost, reliability and accuracy.

Thus, we re-optimised the structure of imidazole/Au(111) for each adsorption site using PBE-D3 and the resulting adsorption energies are shown on the last two lines of Table 1. We note that dispersion corrections slightly alters the equilibrium distance between imidazole and the Au(111) surface for both small and large models. The N–Au distance for the top site shrinks from 2.30 Å to 2.26 Å when using empirical corrections.

However, the dispersion corrections have a much larger impact on the adsorption energies, as can be seen in Table 1. For both slab models, the magnitude of adsorption energy increases up to twofold for some sites (bridge, FCC and HCP). The top site remains the lowest energy adsorption site and the energetic ordering of the sites is preserved (top > bridge > HCP > FCC) for both slab models. This is in agreement with most previous theoretical studies.[30-31] We also note that going from a small slab model to a large model does influence the adsorption energy as was the case previously, but without the same consistent trend. As can be seen from Table 1, the top and HCP sites have larger adsorption energies while the bridge and FCC sites have slightly smaller adsorption energies for the large slab model. However, these remain small relative changes in all cases.

In a recent publication, Wright *et al.*[32] computed a reference adsorption energy for imidazole adsorbed on a top site of Au(111) of –54.1 kJ mol^{-1} and a distance $d_{N–Au}$ = 2.51 Å using a dispersion-corrected functional (vdW-DF/revPBE), a plane waves basis set (25 Ry cut off) and ultra-soft pseudo potentials. The authors have noted that vdW-DFT does tend to overestimate equilibrium separations, which seem to be consistent with our calculations. However, their reported binding energy is roughly half the value we computed using PBE-D3, which could indicate an overestimation of the dispersion correction in the D3 approach. Reckien *et al.*[33] also commented on noticeable overestimations of adsorption energies seen when using standard D3 corrections, and that three-body corrections could provide a more reliable estimate for this quantity. Unfortunately, this is currently beyond the scope of our present study.

3.3. Charge density difference analysis

In order to observe more clearly the interaction between the imidazole molecule and the Au(111) surface, we have calculated the charge density difference (CDD) for the imidazole molecule at different adsorption sites for the large Au(111) surface model (30 Au atoms/layer). The CDD is defined as:

$$\Delta\rho = \rho_{\mathrm{adsorbate@slab}} - \rho_{\mathrm{slab}} - \rho_{\mathrm{adsorbate}},$$

where $\rho_{adsorbate@slab}$ is the charge density of the adsorbate system; ρ_{slab} and $\rho_{adsorbate}$ are the charge densities of the non-interacting slab and that of the adsorbate, respectively. In Fig.9 we show the CDD plots obtained for the four possible adsorption sites (top, bridge, FCC, HCP) where red and blue isosurfaces represent electron charge accumulation and depletion, respectively.

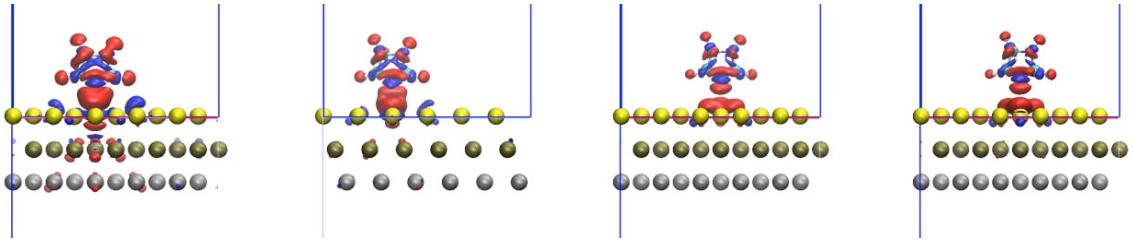

Fig.9 Charge density difference plots for the imidazole molecule adsorbed on a top site (left), bridge site, FCC site and HCP site (right) of the large Au(111) surface model (30 Au atoms/layer). Regions of accumulation/depletion are marked in blue/red, respectively. *Isosurface value* = ± *0.006 e Å*$^{-3}$

The patterns of the CDDs in Fig. 9 show two types of interactions: continuous density-rich zones between the N atom of imidazole and the Au surface (seen for the top site and the bridge site) and density-rich zones that exhibit a clear discontinuity along the N–Au axis (seen for FCC and HCP sites). Continuous zones are usually associated with strong directional bond formation, which is consistent with both top and bridge sites being stronger adsorption sites. Conversely, discontinuous CDDs are associated with less directional bonds that are usually weaker, again consistent with both FCC and HCP being less favourable adsorption sites for imidazole.

We used the same isosurface value to compute all CDD in order to enable a fair comparison between each adsorption site. Interestingly, the CDD of the top site shows that imidazole has a strong influence on the Au(111) surface as each layer is contributing density towards the N–Au bond. This is less apparent for the CDDs from the other adsorption sites, and could further evidence the weaker bonding for the other three adsorption sites. Finally, there appears to be practically no change between the charge density difference plots of imidazole on the HCP site and on the FCC site. This might be one of the reasons why the adsorption energies on both sites are very close.

In summary, we can rationalise the stronger electronic interaction between the imidazole and Au(111) surface by analysing the CDD plots; while no significant energy difference between adsorbate hollow sites (FCC and HCP) can be observed.

Conclusion

We have studied the adsorption of an imidazole molecule at the four main adsorption sites of the Au(111) surface using two different surface models. We used periodic first-principles density

functional theory and the PBE exchange correlation functional to determine adsorption energies with and without dispersion corrections. We find that the adsorption energies determined using the large surface model do not differ much from those determined using the small surface model. However, we note significant qualitative differences for the adsorption geometry at the top site, where the small surface model shows artificial interactions between the adsorbed molecule and its periodic images that force the molecule to adopt an unusual –45° tilt. This indicates that large surface models should be preferred for artifact-free determination of single-molecule adsorption geometries. We further observe that the empirical D3 corrections nearly double the adsorption energy of imidazole compared to uncorrected PBE values, but that the energetic ordering of the sites is preserved. However, the standard D3 approach seems to overestimate adsorption energies compared to other van der Waals correction methods. Finally, charge density difference plots provide a useful analysis of bonding between imidazole and Au(111) and help rationalise the binding difference between the top/bridge adsorption sites and the FCC and HCP sites.

Acknowledgements

This work was carried out in the context of the European PF7 Marie Curie IRSES-GA-2012-317544 Project CapZeo. The authors acknowledge the support of CNRST/MAGRID (http://www.magrid.ma) for providing computing resources on the Moroccan Grid Infrastructure.

References

(1) Barth, J. V.; Brune, H.; Ertl, G.; Behm, R. J. Scanning tunneling microscopy observations on the reconstructed Au(111) surface: Atomic structure, long-range superstructure, rotational domains, and surface defects. Phys. Rev. B. 1990, 42, 9307-9318.

(2) Esken, D.; Turner, S.; Lebedev, O. I.; van Tendeloo, G.; Fischer, R. A. Au@ ZIFs: stabilization and encapsulation of cavity-size matching gold clusters inside functionalized zeolite imidazolate frameworks, ZIFs. Chem. Mater. 2010, 22, 6393-6401.

(3) Li, Z.; Zeng, H. C. Surface and Bulk Integrations of Single-Layered Au or Ag Nanoparticles onto Designated Crystal Planes {110} or {100} of ZIF-8. Chem. Mater. 2013, 25, 1761-1768.

(4) Liu, B.; Smit, B. Molecular Simulation Studies of Separation of CO2/N2, CO2/CH4, and CH4/N2 by ZIFs. J. Phys. Chem. C, 2010, 114, 8515-8522.

(5) Keskin, S. Atomistic Simulations for Adsorption, Diffusion, and Separation of Gas Mixtures in Zeolite Imidazolate Frameworks. J. Phys. Chem. C, 2010, 115, 800-807.

(6) Phan, A.; Doonan, C. J.; Uribe-Romo, F. J.; Knobler, C. B.; O'keeffe, M.; Yaghi, O. M. Synthesis, structure, and carbon dioxide capture properties of zeolitic imidazolate frameworks. Acc. Chem. Res., 2010, 43, 58-67.

(7) Tran, U. P. N.; Le, K. K. A.; Phan, N. T. S. Expanding applications of metal− organic frameworks: zeolite imidazolate framework ZIF-8 as an efficient heterogeneous catalyst for the knoevenagel reaction. ACS Catal., 2011, 1, 120-127.

(8) Grimme, S.; Antony, J.; Ehrlich, S.; Krieg, H. A consistent and accurate ab initio parametrization of density functional dispersion correction DFT-D) for the 94 elements H-Pu . J. Chem. Phys., 2010, 132, 154104-1_154104-19
(9) VandeVondele, J.; Krack, M.; Mohamed, F.; Parrinello, M.; Chassaing, T.; Hutter, J. Quickstep: Fast and accurate density functional calculations using a mixed Gaussian and plane waves approach. Comp. Phys. Comm., 2005, 2, 103-128.
(10) CP2K, http://www.cp2k.org.
(11) Hohenberg, P.; Kohn, W. Inhomogeneous Electron Gas. Phys. Rev. B, 1964, 136, B864-B871.
(12) Kohn, W.; Sham, L. J. Self-Consistent Equations Including Exchange and Correlation Effects. Phys. Rev., 1965, 140, A1133- A1138.
(13) Lippert, G.; Hutter, J.; Parrinello, M. A hybrid Gaussian and plane wave density functional scheme. Mol. Phys., 1997, 92, 477-487.
(14) Hartwigsen, C.; Goedecker, S.; Hutter, J. Relativistic separable dual-space Gaussian pseudopotentials from H to Rn. Phys. Rev. B, 1998, 58, 3641-3662.
(15) Perdew, J. P.; Burke, K.; Ernzerhof, M. Generalized Gradient Approximation Made Simple. Phys. Rev. Lett., 1996, 77, 3865-3868.
(16) VandeVondele, J.; Hutter, J. Gaussian basis sets for accurate calculations on molecular systems in gas and condensed phases. J. Chem. Phys., 2007, 127, 114105-1_114105-9.
(17) VandeVondele, J.; J.; Hutter, An efficient orbital transformation method for electronic structure calculations. J. Chem. Phys., 2003, 118, 4365-4369.
(18) Mavrikakis, M.; Stoltze, P.; Nørskov, J. K. Making gold less noble. Catal. Lett., 2000, 64, 101-106.
(19) Dal Corso, A.; Ab initio phonon dispersions of transition and noble metals: effects of the exchange and correlation functional. J. Phys.; Condens. Matter, 2013, 25, 145401-145410.
(20) Whitman, L. J.; Stroscio, J. A.; Dragoset, R. A.; Celotta, R. J. Geometric and electronic properties of Cs structures on III-V (110) surfaces: From 1D and 2D insulators to 3D metals. Phys. Rev. Lett., 1991, 66, 1338-1341.
(21) M. Mavrikakis, L.B. Hansen, J.J. Mortensen, B. Hammer and J.K. Nørskov, in: Transition State Modeling for Catalysis, ACS Symposium Series, Vol. 721, eds. D.G. Truhlar and K. Morokuma (Am. Chem. Soc., Washington, DC, 1999) ch. 19, p. 245.
(22) Yildirim, H.; Greber, T.; Kara, A. Trends in Adsorption Characteristics of Benzene on Transition Metal Surfaces: Role of Surface Chemistry and van der Waals Interactions. J. Phys. Chem. C, 2013, 117, 20572-20583.
(23) Loo, B. H.; Tse, T.; Parsons, K.; Adelman, C.; EL-Hage, A.; Lee, Y. G. Surface-enhanced Raman spectroscopy of imidazole adsorbed on electrode and colloidal surfaces of Cu, Ag, and Au. J. Raman Spectrosc, 2006, 37, 299-304.
(24) Hoefling, M.; Iori, F.; Corni, S.; Gottschalk, K. E. The Conformations of Amino Acids on a Gold(111) Surface. ChemPhysChem., 2010, 11, 1763-1767.
(25) Iori, F.; Corni, S.; Felice, R. D. Unraveling the Interaction between Histidine Side Chain and the Au(111) Surface: A DFT Study. J. Phys. Chem. C., 2008, 112, 13540-13545.
(26) Cordero, B.; Gómez, V.; Platero-Prats, A. E.; Revés, M.; Echeverría, J.; Cremades, E.; Barragán, F.; Alvarez, S. Covalent radii revisited. Dalton Trans., 2008, 21, 2832-2838.
(27) Bondii, A. van der Waals Volumes and Radii. Phys. Chem., 1964, 68, 441-451
(28) Kovačević, N.; Kokalj, A. DFT Study of Interaction of Azoles with Cu(111) and Al(111) Surfaces: Role of Azole Nitrogen Atoms and Dipole–Dipole Interactions. J. Phys. Chem. C, 2011, 115, 24189-24197.
(29) Chwee, T. S.; Sullivan, M. B. Adsorption studies of C6H6 on Cu (111), Ag (111), and Au (111) within dispersion corrected density functional theory. Chem. Phys., 2012, 137, 134703-1_134703-8.

(30)Fartaria, R. S.; Freitas, F. F. M. : Fernandes, F. M. S. S. A force field for simulating ethanol adorption on Au(111) surfaces. A DFT study. Int. J. Quantum Chem., 2007, 107, 2169-2177.
(31)Bilic, A.; Reimers, J. R.; Hush, N. S. Adsorption of pyridine on the gold(111) surface: Implications for 'alligator clips' for molecular wires. J. Phys. Chem. B, 2002, 106, 6740-6747.
(32)Wright, L. B.; Rodger, P. M.; Corni, S.; Walsh, T. R. GolP-CHARMM: First-Principles Based Force Fields for the Interaction of Proteins with Au(111) and Au(100). Chem J. Chem. Theory Comput., 2013, 9, 1616-1630.
(33)Reckien, W.; Eggers, M.; Bredow, T. Theoretical study of the adsorption of benzene on coinage metals. Beilstein J. Org. Chem., 2014, 10, 1775-1784.